Article

Transmission Characteristics of Adaptive Compensation for Joint Atmospheric Turbulence Effects on the OAM-Based Wireless Communication System

Jingxuan Yang [1,2,*], Hu Zhang [1,3,*], Xiaoguang Zhang [1], Hui Li [1] and Lixia Xi [1]

[1] State Key Laboratory of Information Photonics and Optical Communications, Beijing University of Posts and Telecommunications, Beijing 100876, China; xgzhang@bupt.edu.cn (X.Z.); lihui1206@bupt.edu.cn (H.L.); xilixia@gmail.com (L.X.)

[2] College of Electrical Information, Langfang Normal University, Langfang 065000, China

[3] School of Ethnic Minority Education, Beijing University of Posts and Telecommunications, Beijing 100876, China

* Correspondence: yangjingxuan@bupt.edu.cn (J.Y.); zhh309@bupt.edu.cn (H.Z.)

check for updates

Abstract: Atmospheric turbulence has an impact on the transmission of electromagnetic vortex waves with an orbital angular momentum (OAM) mode. In this paper, based on the joint atmospheric turbulence model, we examine the influence of atmospheric turbulence on the transmission of electromagnetic vortex waves. First, a mathematical model is established to formulate the transmission characteristics of electromagnetic vortex waves under joint atmospheric turbulence. Subsequently, in order to mitigate the influence of the atmospheric turbulence on the electromagnetic vortex waves, an adaptive compensation on phase is proposed. Finally, we analyzed the transmission performance of an OAM-mode multiplexing system using an adaptive compensation method through the wireless communication channel. By means of numerical simulation, the effect of atmospheric turbulence on the transmission characteristics and mode crosstalk of OAM is analyzed. The simulation results show that electromagnetic vortex waves could perform well on the wireless communication system with a low mode crosstalk, which provides the theoretical support to optimizing the mode division multiplexing technology in a free space communication system.

Keywords: electromagnetic vortex wave; orbital angular momentum; wireless communication; adaptive compensation

1. Introduction

It is well known that spectrum resource constraints and channel capacity are increasingly inadequate for the development of wireless communication systems, and how to correctly and reasonably use the existing spectrum resource has become a hot issue. Existing multiplexing technologies, such as frequency division multiplexing, time division multiplexing and polarization multiplexing, are unable to meet future demands of information communication [1]. Space division multiplexing is a new technology that can effectively solve the problem of spectrum tension [2,3]. For free space wireless communication, we used the properties of vortex beam to realize space-division multiplexing. It could provide orbital angular momentum (OAM) with a new degree of freedom, besides amplitude, frequency, and phase. The intrinsic state of OAM can be represented by a quantized topological charge number, and the variety of topological charge number could lead to many kinds of the radial mode and phase distribution. Theoretically, electromagnetic vortex wave can carry infinite

OAM modes at the same frequency, and each OAM mode is orthogonal to each other. Therefore, the application of electromagnetic vortex wave in free-space communication has the unique advantages of high-spectrum utilization and anti-interference. On the basis of OAM-mode multiplexing, a new dimension could be used by the orthogonality of the OAM mode as the basis of multichannel multiplexing [4–6]. However, it is important to consider how to realize multiplexing of a multi-vortex beam, a change of OAM mode after transmission through a turbulent channel, and the mode crosstalk problem caused by multiplexing among various beams [7]. Research on and application of the vortex beams have recently generated great research interest, which has resulted in a new branch of vortex beams in wireless communication systems.

In 1992, Allen and Beijersbergen found that the Laguerre–Gaussian beam could carry an OAM mode [8], and the application of vortex beams in communication has attracted much attention. In 2004, Gibson et al. successfully demonstrated the free space optical (FSO) communication based on OAM sending and receiving data [9]. Later, Pfeifer et al. [10] experimentally produced this beam with a computer-generated hologram (CGH) displayed on a spatial light modulator. Subsequently, Gbur et al. used multiple phase screen simulation technology for studying the topology of vortex beam propagation in atmospheric turbulence, pointing out that a vortex beam carrying the OAM mode through atmospheric turbulence has greater robustness [11]. Erkmen et al. found that a spectrum efficiency can be achieved of 25.6 (bit/s)/Hz with OAM multiplexing. Tyler and Boyd found the pure vortex beam carrying OAM transmissions through free space communication systems, by the propagation in the receiving port and the function between the difference intensity of atmospheric turbulence [12]. Jiang et al. discussed the expansion of the spiral spectrum of the Laguerre–Gaussian beam in the non-Kolmogorov turbulence [13]. Further, Padgett proposed that the divergence of the OAM mode was related to the beam waist type [14]. In 2016, Chen studied the damage to the radial distribution of the Laguerre–Gaussian beam carrying OAM mode with weak-to-strong atmospheric turbulence [15]. The results show that the turbulence induces signal fading, and crosstalk deterioration even leads to link interruption. Therefore, it is necessary to develop a method to compensate the effects of atmospheric turbulence on spatial communication channels. The adaptive compensation theory was first proposed by Babcock in 1953; under ideal conditions, the distorted wavefront can be recovered using this method [16]. Then, the method entered the laboratory experiment stage, and the system was able to improve the communication quality with small initial power after correction. Afterwards, the system operation effect was optimized by the algorithm optimization.

In this article, the basic principle, generation, transformation and application of vortex beams are briefly summarized, as well as their development. We discuss the effects of joint atmospheric turbulence on Laguerre–Gaussian beam transmission. Based on the joint atmospheric turbulence model, a numerical analysis method is used to analyze the crosstalk of OAM mode transmission in a space optical communication system. Then, the method of adaptive compensation is introduced to the receiving end to compensate for fault and modeling uncertainties when wavefront bias occurs. The results show that the electromagnetic vortex waves could maintain good transmission characteristics in turbulent atmosphere by adopting the method of adaptive compensation. This study provides theoretical support for the wide application of mode multiplexing systems in wireless communication systems.

2. Theoretical Model

2.1. Channel Model

The satellite-to-ground link combined with the joint atmospheric turbulence model is considered, including Kolmogorov turbulence and the non–Kolmogorov turbulence model [17]. According to the actual situation of the free space wireless communication link, the channel model of the turbulence could be divided into two layers based on the altitude. The first layer is 0~6 km in the troposphere, and the second layer is above 6 km in the stratosphere. A bulk of experimental results and theoretical

investigations have shown that the turbulence model in the troposphere meets the Kolmogorov turbulence, which meets the non-Kolmogorov turbulence in the stratosphere. Thus, joint atmospheric turbulence refraction spectra density function $\Phi_n(\kappa, \alpha)$ can be described as follows:

$$\Phi_n(\kappa, \alpha) = \Phi_{n1}(\kappa, \alpha) + \Phi_{n2}(\kappa, \alpha), \tag{1}$$

where function $\Phi_{n1}(\kappa, \alpha)$ is the atmospheric turbulence refraction spectra density of the troposphere, and function $\Phi_{n2}(\kappa, \alpha)$ is the atmospheric turbulence refraction spectra density of the stratosphere. The symbol κ is the magnitude of the spatial frequency vector in rad/m units, and the symbol α denotes the spectral power-law exponent. By introducing the spatial filter function $G(\kappa, \alpha)$, spectra density function in Equation (1) could expand into

$$\begin{cases} \Phi_{n1}(\kappa, \alpha) = 0.033 C_n^2(h) \kappa^{-11/3} G(\kappa, \alpha) \\ \Phi_{n2}(\kappa, \alpha) = 0.036 \overline{C}_n^2(h) \kappa^{-5} G(\kappa, \alpha) \end{cases}, \tag{2}$$

where $C_n^2(h)$ is the generalized atmospheric refractive index structure parameter for Kolmogorov turbulence, which represents the measurement of the refractive index fluctuation with the variety of the altitude h, and $\overline{C}_n^2(h)$ is the generalized atmospheric refractive index structure parameter for non-Kolmogorov turbulence, which is directly associated with turbulence strength. Many influencing factors of atmospheric turbulence, temperature gradient, humidity fluctuations, and the correlation between temperature and humidity fluctuations should be considered. According to References [18,19], the atmospheric refractive index structure parameter $\overline{C}_n^2(h)$ can be estimated in terms of the Hufnagel–Valley model:

$$\begin{aligned} \overline{C}_n^2(h) \quad &= 0.00594 \left(\tfrac{\omega}{27} \right)^2 \left(10^{-5} h \right)^{10} \exp\left(-\tfrac{h}{1000} \right) \\ &+ 2.7 \times 10^{-16} \exp\left(-\tfrac{h}{1500} \right) + C_n^2(0) \exp\left(-\tfrac{h}{100} \right) \end{aligned} \tag{3}$$

where ω is the wind speed, which is usually taken as a value of 20 m/s, and $C_n^2(0)$ represents the altitude $h = 0$.

Because the effects of atmospheric turbulence can be considered as large-scale eddies and small-scale eddies, the individual eddies are independent and do not interact with each other. Then we could get the following expression:

$$G(\kappa, \alpha) = G_x(\kappa, \alpha) + G_y(\kappa, \alpha) \tag{4}$$

Based on the extended Rytov theory [20], the symbols $G_x(\kappa, \alpha)$ and $G_y(\kappa, \alpha)$ represent the large-scale and small-scale filter functions for weak-to-strong turbulence, respectively, and have the following forms:

$$\begin{cases} G_x(\kappa, \alpha) = \exp\left(-\kappa^2 / \kappa_x^2 \right) \\ G_y(\kappa, \alpha) = \kappa^\alpha / \left(\kappa^2 + \kappa_y^2 \right)^{\frac{\alpha}{2}} \end{cases}, \tag{5}$$

where κ_x is the cutoff spatial frequencies under weak-to-strong fluctuations of large-scale eddies, and κ_y is the cutoff spatial frequencies under weak-to-strong fluctuations of small-scale eddies. According to Reference [18], the spatial cutoff frequency for large-scale and small-scale filter functions can be further expressed as

$$\begin{aligned} \frac{L}{k \cdot l_x} &= \frac{1}{\kappa_x} \cong \begin{cases} \sqrt{\frac{L}{k}}, & \sigma_R^2(\alpha), \widetilde{\sigma}_R^2(\alpha) << 1 \\ \frac{L}{k \rho_0(\alpha)}, & \sigma_R^2(\alpha), \widetilde{\sigma}_R^2(\alpha) >> 1 \end{cases} \\ l_y &= \frac{1}{\kappa_y} \cong \begin{cases} \sqrt{\frac{L}{k}}, & \sigma_R^2(\alpha), \widetilde{\sigma}_R^2(\alpha) << 1 \\ \rho_0(\alpha), & \sigma_R^2(\alpha), \widetilde{\sigma}_R^2(\alpha) >> 1 \end{cases} \end{aligned} \tag{6}$$

where L is the distance of the propagation path, k represents the wave number, with λ being the wavelength, $\rho_0(\alpha)$ is the coherent length, l_x is the lower limit of the large-scale eddies, l_y is the upper limit of the small-scale eddies, the functions $\sigma_R^2(\alpha)$ and $\widetilde{\sigma}_R^2(\alpha)$ are the Rytov variance of the Kolmogorov turbulence and non-Kolmogorov turbulence, the spectral power-law can suppose the values $11/3$ and 5 for the Kolmogorov turbulence and non-Kolmogorov turbulence, respectively. The coherent length has the form of

$$\rho_0(\alpha) = \left[\frac{-2^{3-\alpha}\pi^2\Gamma\left(1-\frac{\alpha}{2}\right)k^2 A(\alpha)\overline{C}_n^2}{\Gamma\left(\frac{\alpha}{2}\right)} \right]^{\frac{1}{2-\alpha}}, \tag{7}$$

where $A(\alpha)$ denotes the generalized modified amplitude factor; the expression is defined as

$$A(\alpha) = \frac{1}{4\pi^2}\Gamma(\alpha-1)\cos\left(\frac{\alpha\pi}{2}\right). \tag{8}$$

2.2. Adaptive Compensation

Due to the wavefront distortion phenomenon of electromagnetic vortex waves being transmitted through atmospheric turbulence, both intensity and phase will be distorted. Usually, adaptive correction technology is used to compensate the wavefront distortion of the beam, so as to improve greatly and thereby recover the intensity and phase information of the beam. In this paper, we consider that the group of Laguerre–Gaussian beams carrying OAM mode is used to carry information data, as it has been used in numerous applications after the lab generation was performed in Reference [21]. The field distribution of the Laguerre–Gaussian beam is expressed as

$$\begin{aligned} u(r,\theta,z) &= \sqrt{\frac{2p!}{\pi(p+|l|)!}}\frac{1}{w(z)}\left[\frac{\sqrt{2}}{w(z)}\right]^{|l|}L_p^l\left[\frac{2r^2}{w^2(z)}\right]\exp\left[\frac{-r^2}{w^2(z)}\right] \\ &\times \exp\left[\frac{-ikr^2z}{2\left(z^2+z_R^2\right)}\right]\exp\left[i(2p+|l|+1)\tan^{-1}\frac{z}{z_R}\right]\exp(-il\theta) \end{aligned} \tag{9}$$

where the function $w(z)$ is the diffraction limited spot size of the fundamental Gaussian beam, z is the propagation distance, z_R is Rayleigh range, the symbols p and l are the radial and angular coordinate, respectively, in the z plane.

The amplitude at the transmitting end can be expressed as

$$u(r,\theta,z=0) = \sqrt{\frac{2p!}{\pi(p+|l|)!}}\frac{1}{w_0}\left(\frac{\sqrt{2}r}{w_0}\right)^{|l|}L_p^l\left(\frac{2r^2}{w_0^2}\right)\exp\left(\frac{-r^2}{w_0^2}\right)\exp(-il\theta) \tag{10}$$

By transmitting a certain distance in atmospheric turbulence, the electric field on the observed plane is obtained by the diffraction integral

$$u(r,\theta,z) = -\frac{i}{\lambda z}\exp(ikz)\int\int u(r,\theta,z=0)\exp[\psi(r,\theta,z)]\exp\left[\frac{ik}{2z}(r-\rho)^2\right]\rho d\rho d\varphi, \tag{11}$$

where the function $\exp[\psi(r,\theta,z)]$ is the phase change introduced by atmospheric turbulence. The spatial inhomogeneity caused by atmospheric turbulence will change the structure function, which will lead to a change of OAM mode.

In order to reduce the influence of atmospheric turbulence on electromagnetic waves, an adaptive phase compensation method was introduced. At the receiving end, the correlation coefficient of intensity affected by turbulence is as follows:

$$\begin{cases} c_{n1} = \int\int u(r,\phi)u^*(r,\phi)\exp(-il\phi)\exp[-il(\phi+\Delta\phi)]rdrd\phi \\ c_{n2} = \int\int u(r,\phi)u^*(r,\phi)\exp(-il\phi)\exp[-il(\phi-\Delta\phi)]rdrd\phi \end{cases}, \tag{12}$$

where the symbol $\Delta\phi$ is the phase disturbance for the wavefront caused by atmospheric turbulence. The phase of the Laguerre–Gaussian beam can be expressed as the function $P = \exp(-il\phi)$.

Therefore, the output phase can be calculated by

$$P_{n+1} = P_n + m\Delta P_n(c_{n1} - c_{n2}),\tag{13}$$

where n represents the number of iterations, and m is the gain coefficient. The symbol P_n represents the phase within finite steps iterative computations, then the reconstructed phase can be obtained by Equation (12). The significance of this algorithm is to set the total number of iterations, in order to recover the best phase of the system and minimize the residual difference of phases after multiple iterations, so that we could achieve the best performance of the adaptive compensation system without a wavefront sensor.

$$m_n = \frac{P_{n|n-1}}{\left| P_{n|n-1} - P_{n|n} \right|}\tag{14}$$

The symbol $P_{n|n-1}$ represents the phase ratio within n and $(n-1)$ iteration calculation. When the Laguerre–Gaussian beam propagates in atmospheric turbulence, in order to obtain the weight of a new vortex mode component, the disturbed electric field is decomposed into a series of spiral harmonics with a corresponding coefficient as follows:

$$U(r,\theta,z) = \frac{1}{\sqrt{2\pi}}\sum_{-\infty}^{+\infty} a_l(r,z)\exp(il\theta),\tag{15}$$

where the coefficient $a_l(r,z)$ is given by the integral

$$a_l(r,z) = \frac{1}{\sqrt{2\pi}}\int_0^{2\pi} U(r,\theta,z)\exp(-il\theta)d\theta.\tag{16}$$

Radial integration of the above formula can obtain the relative energy using single OAM mode, as for a finite-aperture receiver with radius R, which has the form of

$$C_l = \int_0^R |a_l(r,z)|^2 r dr.\tag{17}$$

In the conditions of atmospheric turbulence, there is a transfer of energy between the emitted OAM modes, which leads to channel crosstalk. If a single OAM mode with an angle index of l is transmitted, the received optical field after the transmission through turbulent atmospheric channel can now be regarded as a superposition of all OAM modes. Therefore, the signal intensity in the receiving terminal is expressed as

$$C = \sum_l g_l C_l,\tag{18}$$

where g_l is the weight coefficient of the OAM mode of angle index l. Because the OAM pattern is orthogonal, the crosstalk between OAM modes can be described by the following conditional probability.

$$P(l|l_0) = \left| \frac{\langle C|C_l \rangle}{C} \right|^2 = |C_l|^2\tag{19}$$

We use the formal model in calculating the channel capacity. The channel capacity can be calculated by

$$B = \max[H(Y) - H(Y|X)],\tag{20}$$

where X and Y is the input and output OAM mode, respectively, and the symbol H denotes entropy.

3. Simulation and Analysis

In this section, first, we compared the transmission characteristics of electromagnetic vortex wave, which carry the single-mode and the multi-mode of OAM through an ideal channel and a turbulent channel, respectively. Then, the adaptive compensation technology was used to correct the turbulence influence exerted on the electromagnetic wave. Furthermore, we compared the transmission characteristics before and after adding the adaptive compensation. Last but not least, the results of signal-to-crosstalk ratio were given, and after adding adaptive compensation, the trend of communication capacity changing with the number of transmission modes was shown. For simulation analysis, the work was modeled on the Laguerre–Gaussian beam with the wavelength of Ku band sets of 2 cm. We used the example of the Laguerre–Gaussian beam for carrying the OAM mode of $p = 0$, $l = 5$. The received mode intensity and phase distribution of electromagnetic vortex waves are shown in Figure 1. It can be seen from the three-dimensional diagram of the intensity distribution that the strength ring of OAM mode with the same topological charge gradually diffuses in the ideal channel as the transmission distance increases. The phase distribution spirals with the change in transmission distance. At the center of the beam, the intensity is zero and the phase singularity occurs.

(a)   **(b)**   **(c)**
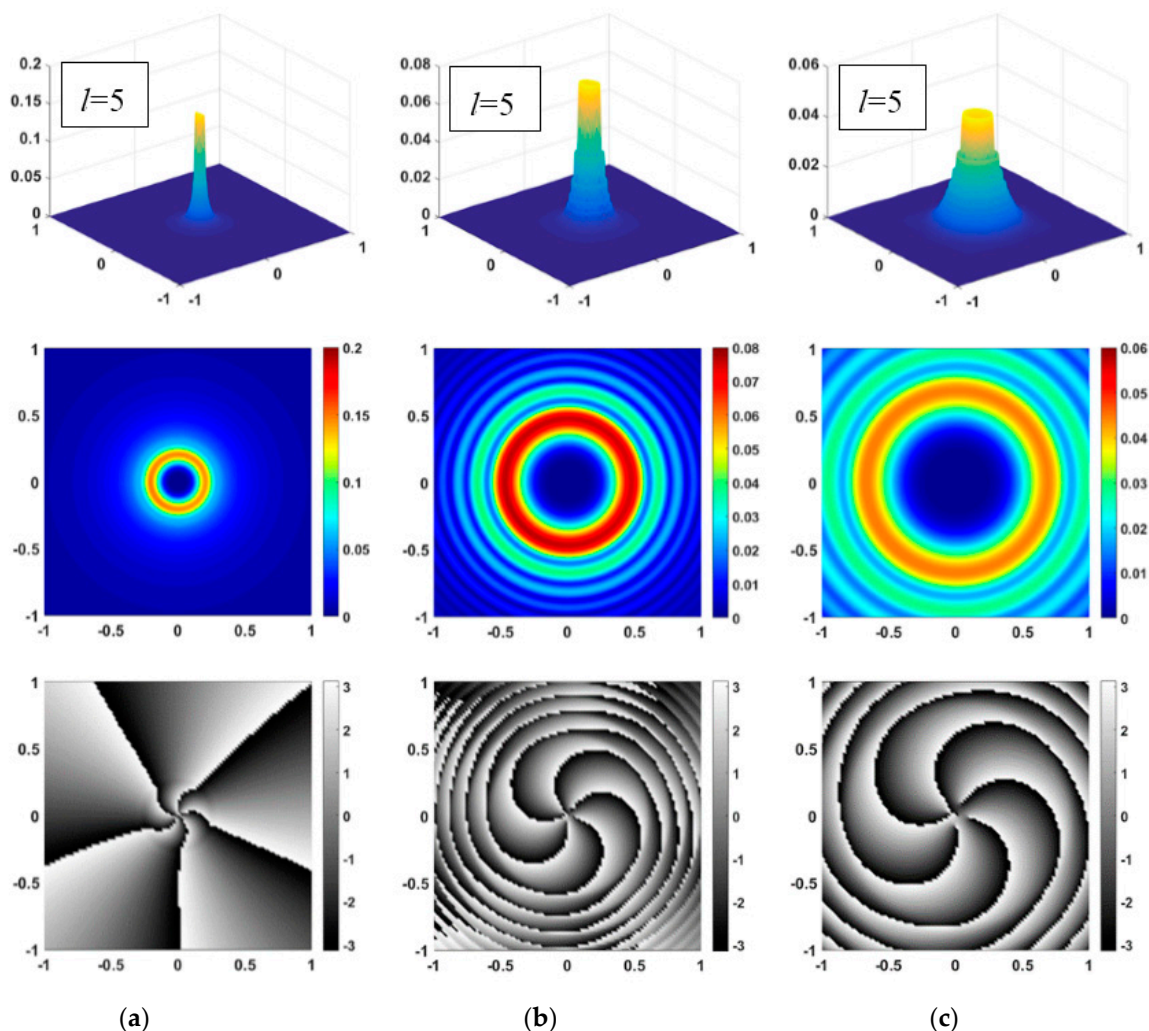
Figure 1. Intensity and phase distribution of electromagnetic vortex waves with transmission distance (**a**) 1 km, (**b**) 5 km, and (**c**) 10 km through ideal conditions.

Due to the atmospheric turbulence in the space communication channel, the spiral wavefront structure of OAM mode was easily distorted by it, which limited the performance of the free space

communication system based on the OAM mode. Therefore, we needed to consider the effect of atmospheric turbulence on electromagnetic vortex waves in free space communication channels. McGlamery was the first to propose a phase screen generation method based on Fourier transform [22]. We can express the changing phase caused by atmospheric turbulence in terms of a Fourier integral. Figure 2 displays the strength of the weak-to-strong atmospheric turbulence by using a series of random phase screens. Some major parameters are as follows: The large-scale $l_x = 10$ m, the small-scale $l_y = 0.01$ m, the length of one side of square phase screen is 0.2 m, and the number of grid points per side is 256. In the simulation process, we used the joint atmospheric turbulence model that corresponded to actual channel conditions.
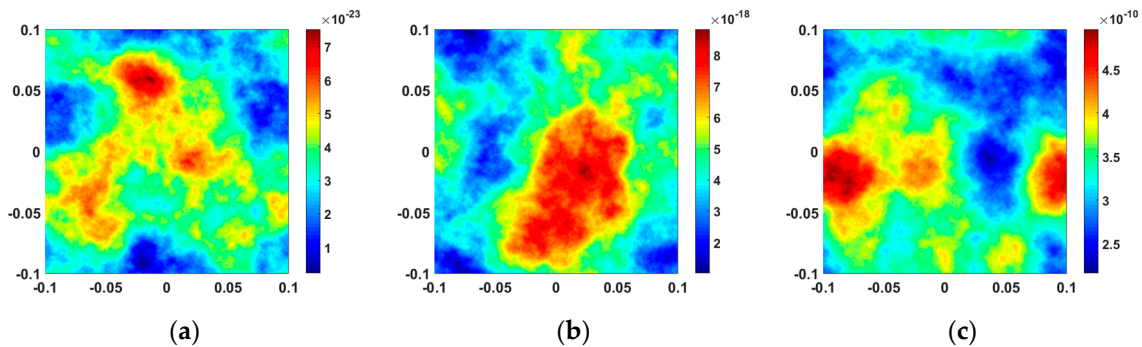
Figure 2. Strength of atmospheric turbulence. (**a**) Weak. (**b**) Moderate. (**c**) Strong.

Electromagnetic vortex wave propagation in the atmosphere channels is affected by a variety of linear and nonlinear effects. The OAM mode is a spatial mode distribution, so the intensity and phase distortion of its wavefront are inevitably affected by atmospheric turbulence. Atmospheric turbulence causes a random fluctuation of the refractive index and distortions of the propagating beam wavefront. Figure 3 shows the intensity and phase distribution of electromagnetic vortex waves with transmission distances of 1 km, 5 km and 10 km under the conditions of moderate-to-strong turbulence. In a single channel transmission, using a single OAM mode, the circular intensity distribution of single mode vortex beam is distorted, and the intensity distribution in the ring is no longer uniform with the increasing propagation distance. The variance of phase distribution is increasingly untidy. Compared to the ideal channel transmission, burr defect appears on the surface of the intensity of electromagnetic vortex waves. The phase perturbation of the single mode vortex beam is gradually distorted, and the isophase lines are distorted by turbulence. The intensity of electromagnetic vortex waves has a weakening trend, and the diameter of the intensity ring gradually diffuses with the increase in propagation distance. The phase diverges outward as the transmission distance increases. In the joint atmospheric turbulence model, the turbulence intensity in the troposphere is greater than that in the stratosphere, so the influence on the phase distribution in the long distance transmission is smaller than that in the short distance transmission below 6 km.

Next, we calculated the crosstalk for each of transmitted OAM modes. Figure 4a–c show histograms of the OAM crosstalk found for 1 km, 5 km and 10 km, respectively. In each of the three cases, we present examples that correspond to the crosstalk generated by transmitting on an isolated channel with $l = 1$, 3, or 5. Each subplot corresponds to a row in topological charge l, such as $l = 1$, and the electromagnetic vortex wave transmits in moderate-to-strong turbulence, the proportion of the dominant mode gradually decreases from 0.898 to 0.180. When the transmission distance increases to 10 km, the dominant mode is submerged by the crosstalk mode. From Figure 4 we can see a trend that transmitted OAM mode transfers energy into the neighboring modes along with transmission distance, and in the case of the weak turbulence, mode crosstalk occurs mainly in adjacent modes, whereas in the case of moderate-to-strong turbulence, mode crosstalk gradually expands to other peripheral modes. Furthermore, for each of the sending OAM modes, the effect of turbulence on mode transmission in turbulence channels is gradually unstable. Under moderate-to-strong turbulence,

because the electromagnetic wave is inevitably influenced by turbulence disturbance, the receiving end cannot correctly identify the mode of transmission. Therefore, the mode crosstalk caused by atmospheric turbulence needs to be compensated for by obtaining the right mode.
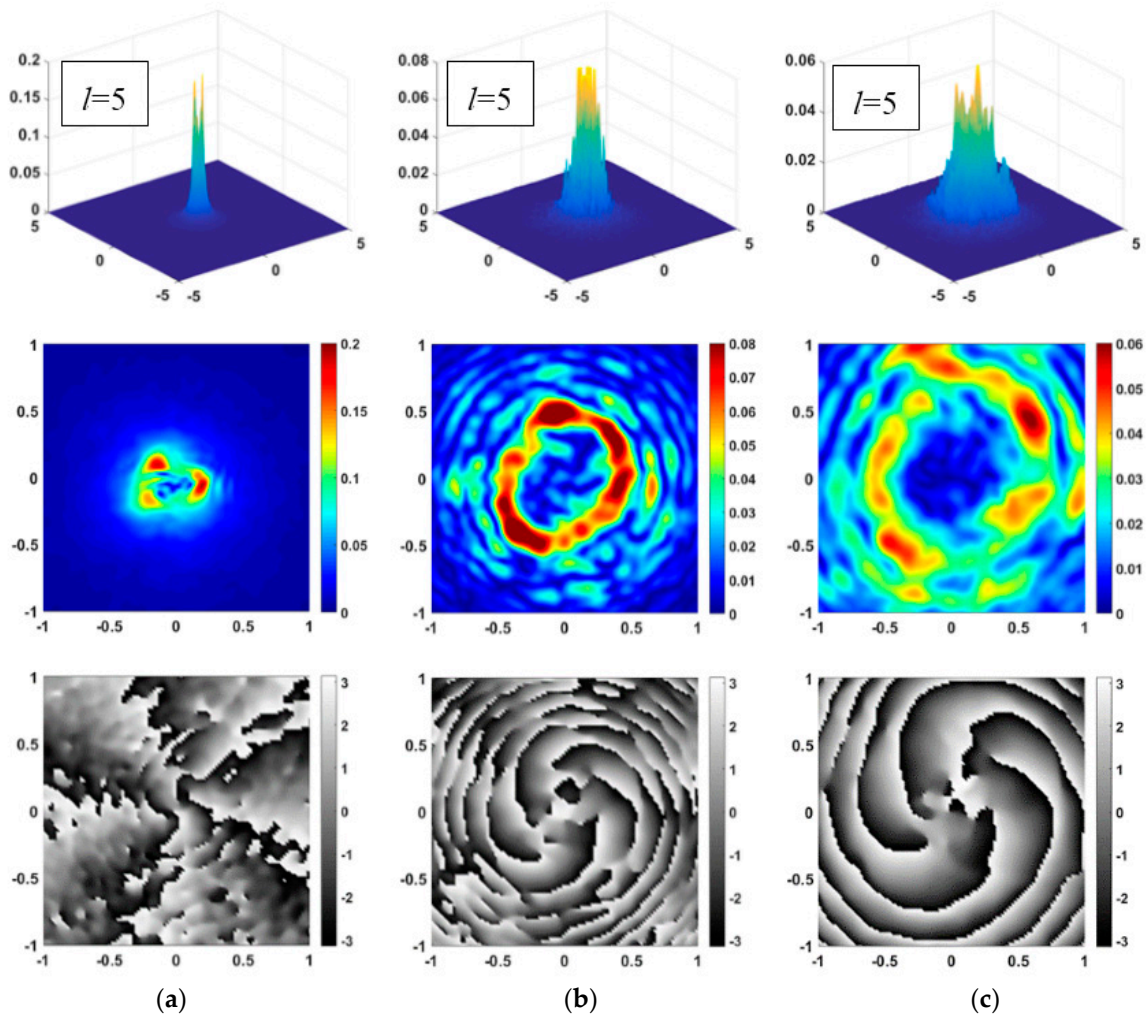
Figure 3. Intensity and phase distribution of electromagnetic vortex waves with the transmission distance (**a**) 1 km, (**b**) 5 km and (**c**) 10 km under moderate-to-strong turbulence conditions.

Because the wavelength of microwave band is much larger than that of light band, the effect of weak turbulence on electromagnetic vortex waves is small. Therefore, only the results of compensation for the influence of moderate-to-strong turbulence on electromagnetic vortex waves are given. Figure 5a–c displays the intensity and phase distribution of electromagnetic vortex waves with adaptive compensation found for 1 km, 5 km and 10 km, respectively. After the adaptive compensation, the intensity of beam increased significantly and the distribution became uniform. The distortion degree of the isophase line was greatly improved, which indicates that the phase distortion is effectively compensated. This shows that the adaptive compensation scheme is very effective for electromagnetic vortex wave distortion correction with a single topological number.
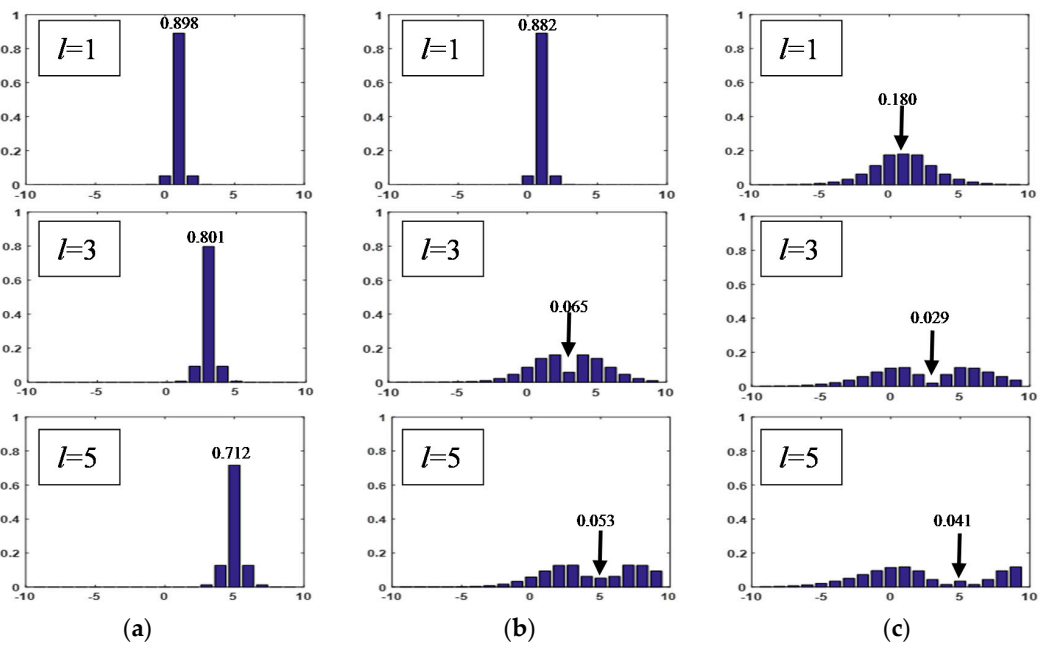
Figure 4. Variance of crosstalk with the transmission distance (**a**) 1 km, (**b**) 5 km and (**c**) 10 km under moderate-to-strong turbulence conditions.
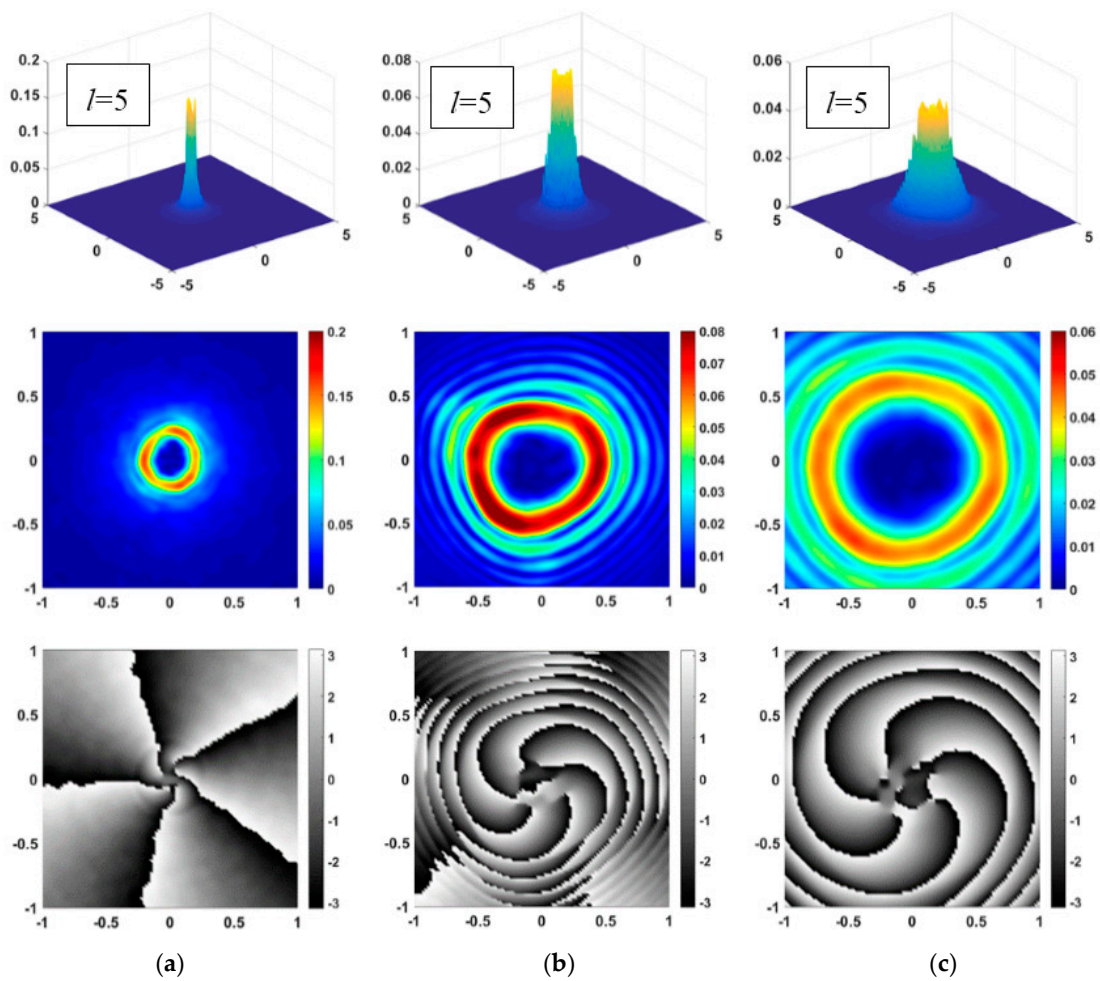
Figure 5. Intensity and phase distribution of electromagnetic vortex waves with transmission distances of (**a**) 1 km, (**b**) 5 km and (**c**) 10 km, with adaptive compensation.

Figure 6a–c show histograms of the OAM crosstalk within adaptive compensation found for 1 km, 5 km and 10 km, respectively. In each of the three cases, we present examples that correspond to the crosstalk generated by transmitting on an isolated channel with $l = 1, 3,$ or 5. Each subplot corresponds to a row in topological charge l, such as $l = 1$, and the electromagnetic vortex wave transmits in moderate-to-strong turbulence. The proportion of the dominant mode gradually decreases from 1 to 0.382. In Figure 6a, when a single OAM mode is compensated for the influence of turbulence by the adaptive compensation method, crosstalk among channels is negligible. In comparing Figure 4b with Figure 6b, when topological charge $l = 1$, the proportion of dominant mode before and after adaptive compensation is increased from 0.882 to 1. Comparing Figures 4c and 6c, when the transmission distance increases to 10 km, the mode of transmission is increased from 0.180 to 0.382, and at this point, the transmitted OAM mode is still the main component after adaptive compensation. For long distance transmission (5 km–10 km), the OAM mode stability becomes worse along with the order number increase of the topological charge l. Therefore, the adaptive compensation can effectively increase the proportion of the main mode, and the crosstalk caused by turbulence can be reduced.
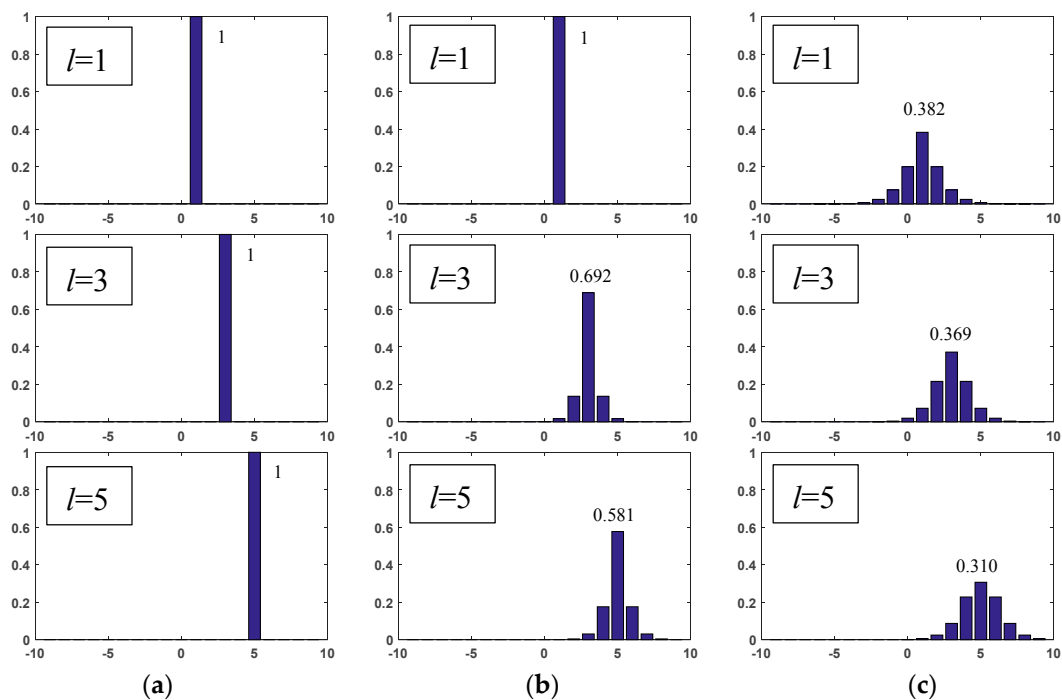
Figure 6. Variance of crosstalk through the weak-to-strong turbulence with transmission distance of (**a**) 1 km, (**b**) 5 km and (**c**) 10 km, with adaptive compensation.

Figure 7 displays the intensity and phase distribution of electromagnetic vortex waves with the transmission distance 1 km, 5 km and 10 km for multiplexing $l = 1, 3, 5$ under moderate-to-strong turbulence conditions. It can be seen from the two-dimensional intensity distribution diagram of OAM beam multiplexing that, in the process of turbulent transmission, the intensity of the electromagnetic vortex waves decreases and the intensity spot diffuses due to the influence of the turbulence effect. The intensity distribution deforms and the power is dispersed gradually with the increasing transmission distance. Due to atmospheric disturbance, the phase distortion of the OAM multiplexed beam is different, and the phase diffuses from the center to the periphery. The isophase lines gradually bend and even blur out of shape, and it is difficult for the receiving end to separate the effective information carried by the OAM mode.
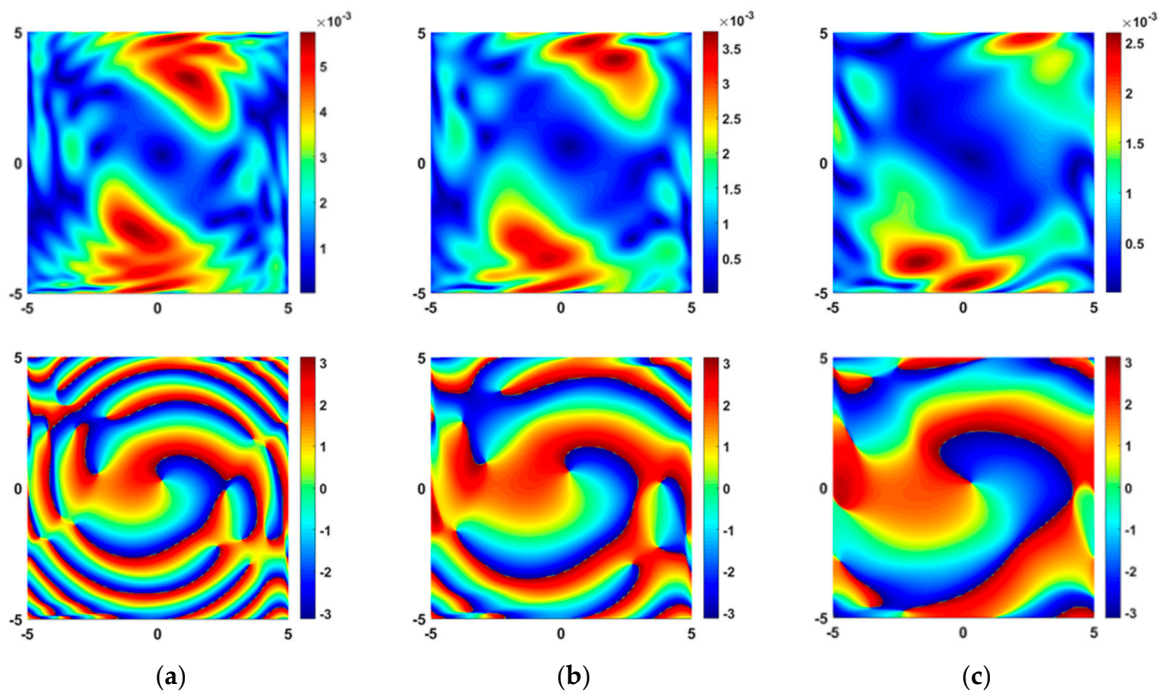
Figure 7. Intensity and phase distribution of electromagnetic vortex waves with the transmission distance (**a**) 1 km, (**b**) 5 km and (**c**) 10 km for multiplexing $l = 1, 3, 5$ under moderate-to-strong turbulence conditions.

For the whole OAM multiplexing system, electromagnetic vortex waves transmitting into the atmosphere will be affected by atmospheric turbulence, so it needs to be compensated to improve the communication quality. With adaptive compensation, the intensity and phase distribution of electromagnetic vortex waves with the transmission distance 1 km, 5 km and 10 km under moderate turbulence conditions are shown in Figure 8. The intensity of multiplexed OAM modes is increased and the shape is restored. The distortion degree of isophase lines are improved, and they become smooth and tidy. Therefore, the intensity and phase effects of atmospheric turbulence on OAM multiplexing can be compensated well by the method of adaptive compensation.

Figure 9 displays the crosstalk distribution of electromagnetic vortex waves with transmission distances of 1 km, 5 km and 10 km under moderate-to-strong turbulence conditions. The first line in Figure 9 is the crosstalk probability distribution of the OAM multiplexed beam transmitted in turbulence. After the transmission of the OAM multiplexed beam through atmospheric turbulence, its purity is damaged. At this time, all the OAM modes are doped with other modes with different topological charges to varying degrees. The singularity occurs when the topological charge is 0. Due to large mode crosstalk among different modes, each beam no longer maintains the original distribution state. Then, the dispersion between adjacent modes is serious, and the proportion of OAM modes with topological charges of 2, 4 and 6 have a high percentage. The second row of graphs in Figure 9 shows the crosstalk distribution of electromagnetic vortex waves with the increasing transmission distance after adaptive compensation. The purity of the OAM mode remains within its own transmission mode, and the crosstalk modes are of smaller proportions. At this moment, the mode information can be judged from the mode of the receiving end.
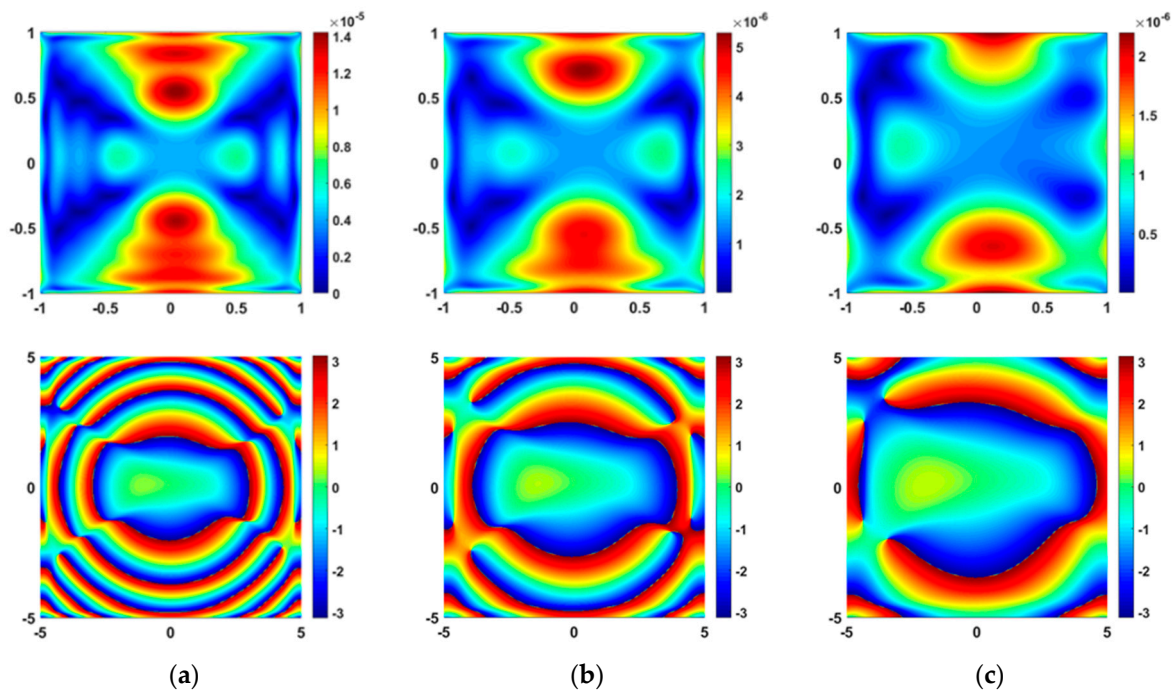
Figure 8. Intensity and phase distribution of electromagnetic vortex waves with transmission distance of (**a**) 1 km, (**b**) 5 km and (**c**) 10 km for multiplexing *l* = 1, 3, 5 under moderate turbulence conditions, with adaptive compensation.
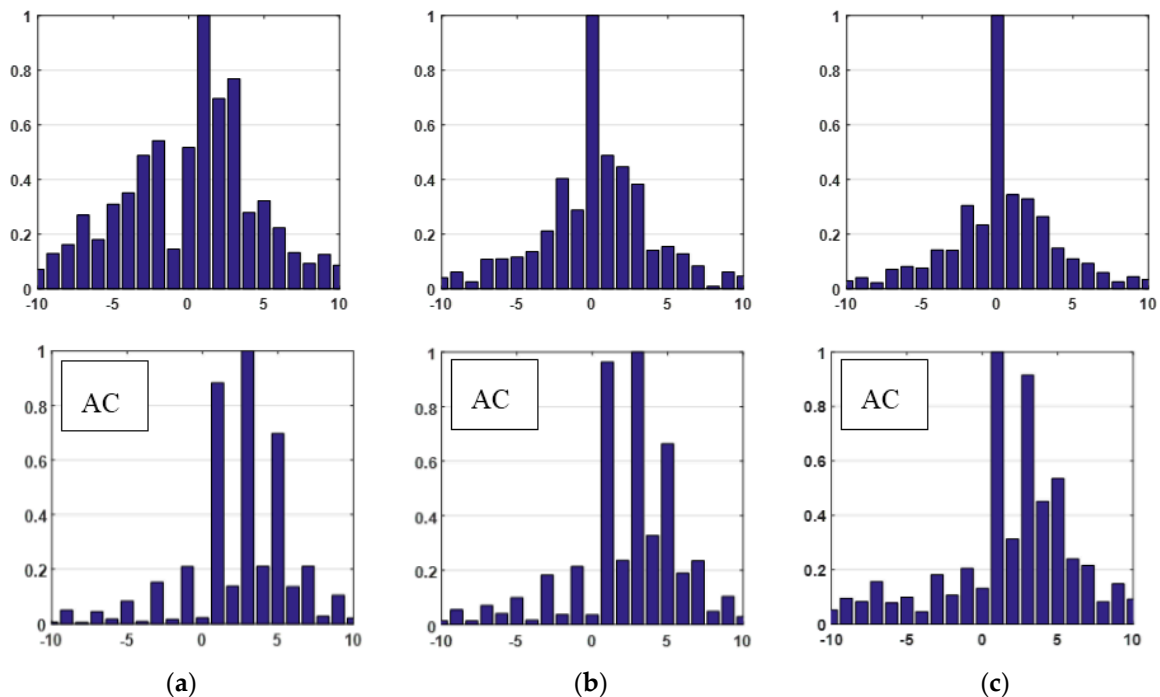
Figure 9. Crosstalk distribution of electromagnetic vortex waves with transmission distance of (**a**) 1 km, (**b**) 5 km and (**c**) 10 km under moderate-to-strong turbulence conditions.

We show the signal-to-crosstalk ratio with transmission path in Figure 10. The signal shows a weakening trend along with the transmission path, whereas the crosstalk shows the opposite trend. In weak atmospheric turbulence, the signal is much larger than crosstalk. Also, under the conditions of the moderate-to-strong turbulence, the ratio of signal to crosstalk is lower than that in weak atmospheric turbulence, but the signal is still the main part (more than 50 dB).
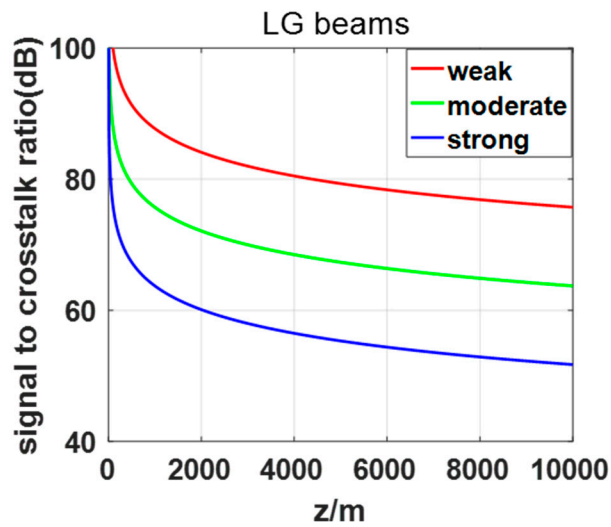
Figure 10. Signal-to-crosstalk ratio with transmission path after adaptive compensation.

In the wireless communication system based on OAM-modes modulation, the atmospheric turbulence will scatter the energy of the transmitted OAM mode into another mode. Figure 11 shows the variance of channel capacity with different OAM modes in weak-to-strong atmospheric turbulence. It is evident that channel capacity increases with the number of transmission OAM modes. In Ku band the channel capacity could reach the ideal situation under weak and moderate atmospheric turbulence, and channel capacity, through the fluctuating of strong atmospheric turbulence, has entered into a downtrend. Thus, we could improve the capacity of the wireless communication system by using vortex electromagnetic waves.
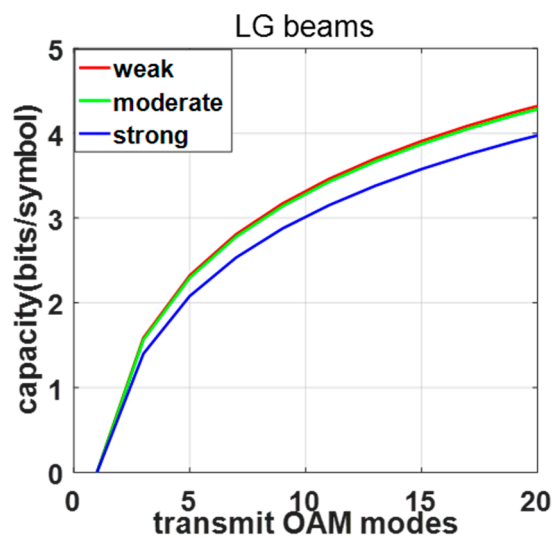
Figure 11. Variance of channel capacity with different OAM modes.

4. Conclusions

In this paper, based on joint atmospheric turbulence, we established a mathematical model for electromagnetic vortex wave transmission in free space communication systems in Ku band. Initially, through theoretical analysis and numerical simulation validation, the intensity and phase of electromagnetic vortex waves were easily distorted by atmospheric turbulence after it was transmitted through a free space channel. Simultaneously, mode crosstalk was obvious, and its own part of the energy was transferred to another OAM mode, making this other OAM mode

carry information that was not pure. Then, moderate-to-strong turbulence induced severe intensity and phase disturbances, which were significantly reduced by the applied adaptive compensation. In addition, with the compensation method, the probability of crosstalk of the OAM mode to the neighboring mode increased; however, the standard mode of receiving was still the main part, which could be accepted. Finally, we used OAM multiplexing technology to realize the multiplexing transmission of information, and the intensity and phase distortion of multiplexing signals caused by the atmospheric turbulence were improved by an adaptive compensation technique. This method can effectively improve the mode crosstalk generated by OAM mode multiplexing, which provides a foundation for the application of module division multiplexing technology. The channel capacity of OAM-based wireless communication links, under the impact of weak-to-strong atmospheric turbulence, is evidently promoted by the increasing number of OAM modes. This study provides a theoretical support for future research on microwave propagation in wireless communication links through weak-to-strong turbulence.

References

1. Willner, A.E.; Huang, H.; Yan, Y.; Ren, Y.; Ahmed, N.; Xie, G.; Bao, C.; Li, L.; Cao, Y.; Zhao, Z.; et al. Optical communications using orbital angular momentum beams. *Adv. Opt. Photonics* **2015**, *7*, 66–106. [CrossRef]
2. Trichili, A.; Salem, A.B.; Dudley, A.; Zghal, M.; Forbes, A. Encoding information using Laguerre Gaussian modes over free space turbulence media. *Opt. Lett.* **2016**, *41*, 3086–3089. [CrossRef] [PubMed]
3. Zhao, S.M.; Leach, J.; Gong, L.Y.; Ding, J.; Zheng, B.Y. Aberration corrections for free-space optical communications in atmosphere turbulence using orbital angular momentum states. *Opt. Express* **2012**, *20*, 452–461. [CrossRef] [PubMed]
4. Čelechovský, R.; Bouchal, Z. Optical implementation of the vortex information channel. *N. J. Phys.* **2007**, *9*, 328–333. [CrossRef]
5. Qin, Z.Y.; Tao, R.M.; Zhou, P.; Xu, X.J.; Liu, Z.J. Propagation of partially coherent Bessel-Gaussian beams carrying optical vortices in non-Kolmogorov turbulence. *Opt. Laser Technol.* **2014**, *56*, 182–188. [CrossRef]
6. Bozinovic, N.; Yue, Y.; Ren, Y.; Tur, M.; Kristensen, P.; Huang, H.; Willner, A.E.; Ramachandran, S. TerabitScale Orbital Angular Momentum Mode Division Multiplexing in Fibers. *Science* **2013**, *340*, 1545–1548. [CrossRef] [PubMed]
7. Cui, Q.; Li, M.; Yu, Z. Influence of topological charges on random wandering of optical vortex propagating through turbulent atmosphere. *Opt. Commun.* **2014**, *329*, 10–14. [CrossRef]
8. Allen, L.; Beijersbergen, M.W. Orbital angular momentum of light and the transformation of Laguerre-Gaussian laser modes. *Phys. Rev. A* **1992**, *45*, 8185–8189. [CrossRef] [PubMed]
9. Gibson, G.; Courtial, J.; Padgett, M.J.; Vasnetsov, M.; Pas'ko, V.; Barnett, S.M.; Franke-Arnold, S. Free-space information transfer using light beams carrying orbital angular momentum. *Opt. Express* **2004**, *12*, 5448–5456. [CrossRef] [PubMed]
10. Pfeifer, R.N.C.; Nieminen, T.A.; Heckenberg, N.R.; Rubinsztein-Dunlop, H. Colloquium: Momentum of an electromagnetic wave in dielectric media. *Rev. Mod. Phys.* **2007**, *79*, 1197. [CrossRef]
11. Gbur, G.; Tyson, R.K. Vortex beam propagation through atmospheric turbulence and topological charge conservation. *J. Opt. Soc. Am. A* **2008**, *25*, 225–230. [CrossRef]
12. Padgett, M.J.; Miatto, F.M.; Lavery, M.P.J.; Zeilinger, A.; Boyd, R.W. Divergence of an orbital-angular-momentum-carrying beam upon propagation. *New J. Phys.* **2015**, *17*, 023011. [CrossRef]
13. Jiang, Y.S.; Wang, S.H.; Zhang, J.H.; Ou, J.; Tang, H. Spiral spectrum of Laguerre-Gaussian beam propagation in non-Kolmogorov turbulence. *Opt. Commun.* **2013**, *303*, 38–41. [CrossRef]

14. Milione, G.; Lavery, M.P.J.; Huang, H.; Ren, Y.; Xie, G.; Nguyen, T.A.; Karimi, E.; Marrucci, L.; Nolan, D.A.; Alfano, R.R.; et al. 4× 20 Gbit/s mode division multiplexing over free space using vector modes and a q-plate mode (de) multiplexer. *Optics Lett.* **2015**, *40*, 1980–1983. [CrossRef] [PubMed]

15. Chen, C.; Huamin, Y. Characterizing the radial content of orbital-angular-momentum photonic states impaired by weak-to-strong atmospheric turbulence. *Opt. Express* **2016**, *24*, 19713–19727. [CrossRef] [PubMed]

16. Babcock, H.W. The possibility of compensating astronomical seeing. *Publ. Astron. Soc. Pac.* **1953**, *65*, 229–236. [CrossRef]

17. Du, W.; Yang, J.; Gong, Q.; Liu, J.; Zhang, G.; Yang, Z.; Ma, J.; Yao, Y.; Lu, J.; Liu, D.; et al. Angle of Arrival Fluctuations for Optical Waves Propagating Through Joint Moderate to Strong Atmospheric Turbulence. *J. Russ. Laser Res.* **2016**, *37*, 82–90. [CrossRef]

18. Andrews, L.C.; Phillips, R.L. *Laser Beam Propagation Through Random Media*; SPIE Press: Bellingham, WA, USA, 2005.

19. Du, W.; Zhu, H.; Liu, D.; Yao, Z.; Cai, C.; Du, X.; Ai, R. Effect of non-Kolmogorov turbulence on beam spreading in satellite laser communication. *J. Russ. Laser Res.* **2012**, *33*, 401–408. [CrossRef]

20. Andrews, L.C.; Phillips, R.L.; Hopen, C.Y. *Laser Beam Scintillation with Applications*; SPIE Press: New York, NY, USA, 2001.

21. Lin, Z.; Chen, X.; Qiu, W.; Pu, J. Propagation Characteristics of High-Power Vortex Laguerre-Gaussian Laser Beams in Plasma. *Appl. Sci.* **2018**, *8*, 665. [CrossRef]

22. Welsh, B.M. Fourier-series-based atmospheric phase screen generator for simulating an isoplanatic geometries and temporal evolution. In *Propagation and Imaging through the Atmosphere*; International Society for Optics and Photonics: New York, NY, USA, 1997; Volume 3125.